Structural Engineering and Mechanics, Vol. 15, No. 1 (2003) 53-70
DOI: http://dx.doi.org/10.12989/sem.2003.15.1.053

New design concept and damage assessment of large-scale cooling towers

Sam-Young Noh† and Konstantin Meskouris‡

Institute for Structural Statics and Dynamics RWTH Aachen, Mies-van-der-Rohe-Strasse 1, D-52056 Aachen, Germany

Reinhard Harte‡

Institute for Statics and Dynamics, Bergische Universität Wuppertal, Pauluskirchstrasse 7, D-42285 Wuppertal, Germany

Wilfried B. Krätzig‡

Institute for Statics and Dynamics, Ruhr-Universität Bochum, Universitätsstrasse 150, D-44780 Bochum, Germany

(Received October 4, 2002, Accepted December 18, 2002)

Abstract. The motivation of this paper is to introduce the modern technology of large-scale cooling tower design. Thereby the innovative design concept for the world's largest cooling tower with a height of 200 m is briefly presented (Harte & Krätzig 2002, Bush *et al.* 2002). The new concept was considered not only for safety, but also for preservation of the durability of the structure, because cracking damage in large cooling towers in general cause extremely high cost of maintenance and repair. The paper demonstrates numerically the damage process in large cooling towers (Krätzig *et al.* 2001), and describes some basics of the numerical finite element approach for damage propagation modelling of shell structure. A prototype is analysed to trace the progressive damage process, whereby the changes in the dynamical behaviour of the structure, as mirrored in its natural frequencies and the corresponding mode shapes, are presented and discussed. Finally, the example shows that such damage processes develop progressively over the life-time of the shell structure.

Key words: cooling tower; FE-simulation; structural damage; material modeling of RC.

1. Introduction

World-wide the knowledge is growing, that the generation of energy has to be accompanied by innovative techniques to preserve resources and to prevent pollution. In this context natural draught cooling towers play a significant role as power plant components. They balance the technical

† Assistant Lecturer
‡ Professor

requirements of an efficient energy supply with appropriate means for protection of the environment. To avoid thermal pollution of rivers, lakes and seashores by using their water for cooling, natural draught cooling towers are the most effective cooling measures by minimizing the need of water. In order to save natural fuel, the degree of efficiency of power plants must be increased. Because of the development of larger power units and thus of higher cooling demand, bigger and bigger cooling towers have been constructed over the last decades. Consequently cooling towers have already exceeded the range of our previous experience. Fig. 1 illustrates the last three cooling tower projects in Germany.

In many exiting cooling towers world-wide, damage phenomena can be observed. After years of damage-free behaviour, visible cracks develop suddenly in the meridional direction of the shell. This crack-damage, initiated by thermal and hygric effects, grows progressively with time. Because of the extremely high costs for maintenance and repair, the preservation and the improvement of the durability as well as achievement of extended life-cycles of such structures are more important issues. To trace the structural response with the progression of deteriorations and damage processes, the numerical tools have to be improved with respect to reliability and efficiency. Finally a durability-oriented design concept is developed, in the following and applied to the case of a 200 m prototype cooling tower.

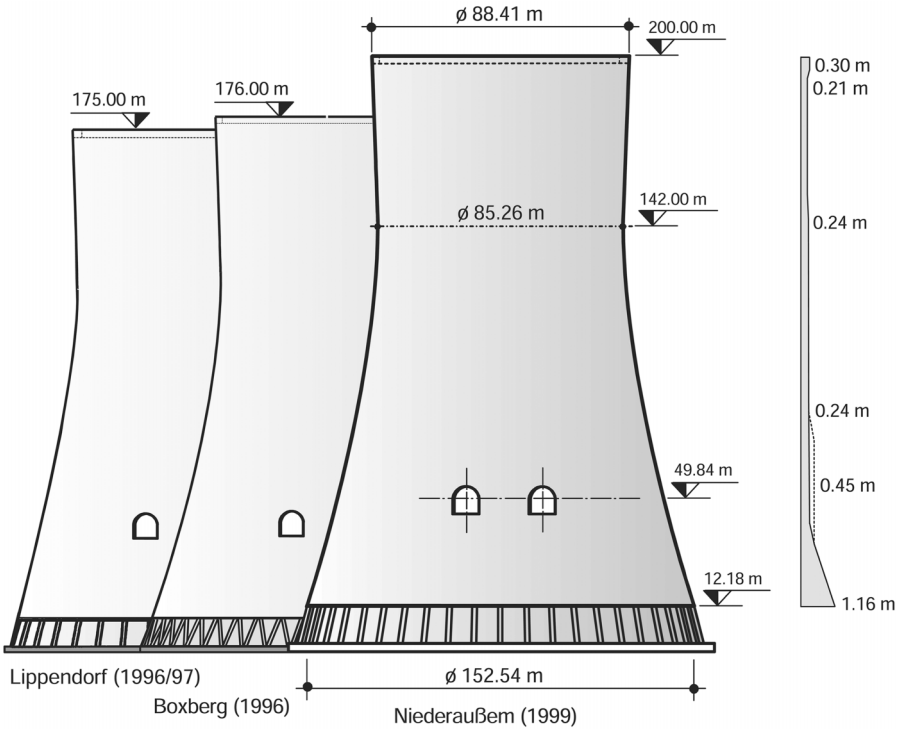

Fig. 1 New cooling tower generation in Germany

2. Modern technology for the construction of large-scale cooling towers

The world's largest cooling tower is shown in Fig 1. It is located in Niederaussem and measures a height of 200 m and a base diameter of 152,5 m with wall thickness varying mostly from 22 to 24 cm. The tower belongs to the new BoA-block at the RWE power station Niederaussem, near Cologne in Germany, a new lignite power unit with 965 MW net electric capacity. It consists of highly innovative new technologies, in order to achieve a net degree of efficiency of more than 43% which referents the highest value for a fossil fuel power plant.

The behaviour of such large towers can not be considered by extrapolating the behaviour of smaller ones. Especially the natural frequencies will drop with height leading to increasing dynamic amplification under wind action and thus to more severe dynamic deterioration than experienced up to now.

The new design concepts for the world's largest cooling tower in Niederaussem (Fig. 2), described in Harte & Krätzig (2002) in detail, can be summarized as follows:

- A form optimization process yielded an optimal shape of the shell for the best possible load bearing behaviour.
- Extensive vibration studies and stability calculations have been carried out for optimizing the shell thickness over shell's height.
- A realistic wind distribution considering interference effect, caused by the existing power units in the surrounding, was determined by a series of wind tunnel tests carried out by the Ruhr University Bochum.
- The distribution of soil characteristics yielded non-axisymmetric stress distributions with a great influence on the whole structure.
- The structural behaviour of the tower due to the cleaned flue-gas injection in a high position of the shell with two openings with a diameter of approx. 10 m was additionally analysed (Fig. 2). Because of the heavy loads from the pipes on the shell wall, each 2000 kN vertically and ±400

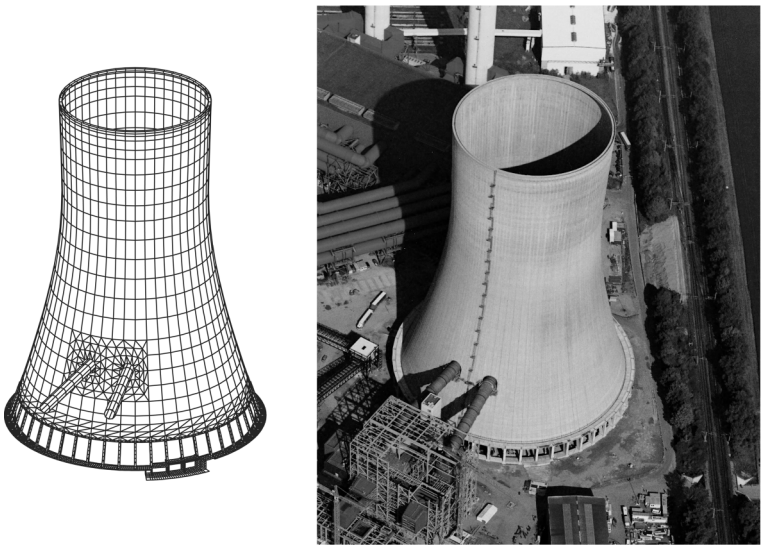

Fig. 2 FE-mesh and completed Niederaussem-tower (Source RWE)

kN horizontally, and a considerable influence of the openings on the global vibration and stability behaviour of the cooling tower shell, partial stiffening of the shell wall up to 45 cm in the vicinity of the openings was done to sufficiently restore the original buckling strength.

- Acid resistance and extended durability were ensured by developing a new concrete mixture, termed SRB 85/35. The compact packing of the aggregate due to Fuller-Thompson sieve-curve combined with fly-ash and microsilica additives yielded a high performance concrete C 70/85 (Busch *et al.* 1999) with a compression strength close to 85 MN/m^2 according to European Standards EC 2, whereas the stiffness and the tensile strength correspond to those of normal concrete C 35/45. The lower stiffness and tensile strength are very advantageous for the limitation of thermal stresses and expected crack-widths.
- An additional component of the durability-oriented design was to reduce cracking-sensitivity of the upper parts of the shell due to wind vibration by means of pre-stressing the U-shaped upper edge ring. This will avoid early cracking and thus improve the dynamic properties of the shell, which is especially efficient for the preservation of durability in the damage process, as will be discussed in section 4.
- Standard structural analysis and design have been performed for ultimate limit states and serviceability limit states with the restriction of average crack-width $w_m \leq 0.2$ mm.
- Verification of the global safety by non-linear collapse analyses yielded the ultimate load level of 2.54 times of design wind load.

3. Damage analysis of large-scale cooling towers

In the following the numerical damage analysis in the context of finite element analysis will demonstrate the damage process of large cooling towers. The accumulation of damages is a non-linear process which cannot be covered by the usual static calculation techniques: Damage simulations should reproduce the load-bearing behaviour of structures as realistically as possible, taking into account the true load process as well as a realistic material modelling.

The finite shell element used for the analysis has 4 nodes and is formulated within a finite rotation shell theory with constant transverse deformation, according to Reissner-Mindlin (Menzel 1996). The geometry of fundamental and deformed configuration are approximated isoparametrically through bilinear polynomials. To avoid shear-locking, the transverse shear strains are linearly interpolated in the sense of an assumed strain element at the collocation points.

The material non-linearity is implemented by means of a multi-layered model and, as shown in Fig. 3, the reinforced concrete in the tower shell is modelled as a layered continuum of uniaxial layers of reinforcement steel and of plane stress layers of concrete. The constitutive information in a material point has to be transformed upwards to the finite element level and further to the structure level. This homogenisation concept is efficiently realized by a multi-level simulation technique (Krätzig 1997).

3.1 Material model of reinforced concrete

Reinforced concrete is a composite material consisting of concrete and reinforcement steel, and its load-carrying behaviour is highly non-linear. Characteristic properties of concrete are an essentially non-linear stress-strain relationship under monotonic loading, yielding and damage development

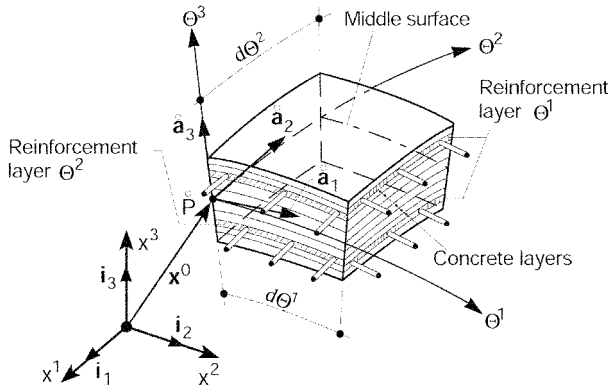

Fig. 3 Multi-layered reinforced concrete shell model

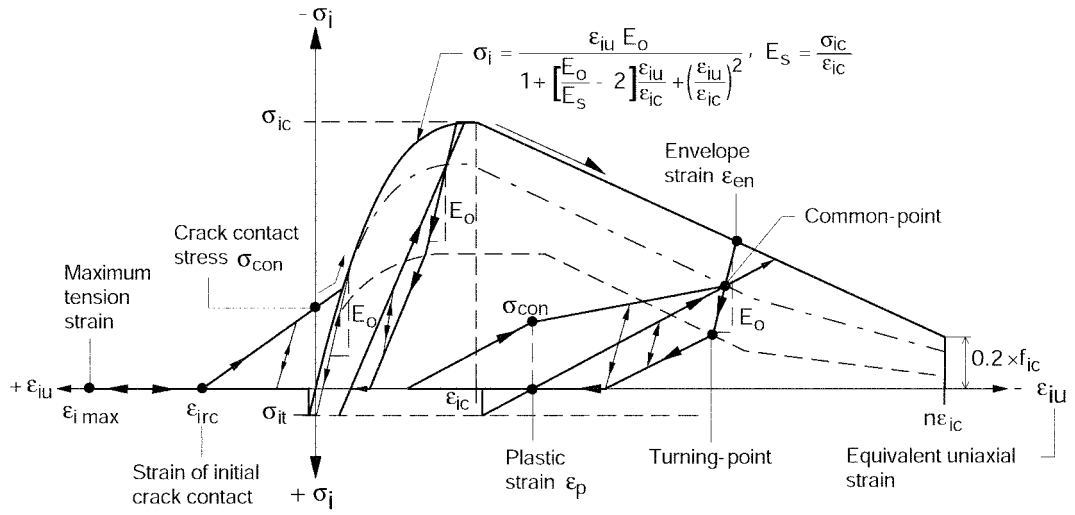

Fig. 4 Constitutive law of concrete in principal stress system

under cyclic loading in the compression domain, and also cracking and crack closing processes in the tension domain. Compared to concrete, the linear elasto-plastic material law of reinforcing steel is quite simple. In addition, however, the complex non-linear bonding behaviour between concrete and steel as well as the tension-stiffening effect (participation of the concrete between cracks for monotonic and cyclic loading) are phenomena which must be considered. The material model summarized in the following was presented by Noh (2001) in detail.

3.2 Concrete model

The concrete model shown in Fig. 4 goes back to Darwin & Pecknold (1974) and has then been improved by several researchers including the authors. In modern terminology, it describes a non-linear elasto-plastic damage model with a softening range. Since it is based on one- and two-

dimensional experiments, originally on those of Karsan & Jirsa (1969) and Kupfer *et al.* (1969), its character is rather empirical. It is exactly this property that makes it attractive for theoretical, normative and experimental additions. A discussion of the model can be found in Noh *et al.* (2002).

The characteristics of the formulation are

- Applicability for monotonic and cyclic load processes with only four material parameters, namely the tension strength f_{ct}, compression strength f_c, the strain for the compression strength ε_c and the initial Young's modulus E_0.
- Yield conditions are based on the experimental results of Kupfer *et al.* (1969).
- Cyclic behaviour in compression is formulated based on the experimental data of Karsan & Jirsa (1969) regarding degradation of strength and stiffness, yielding and energy dissipation.
- The ultimate failure criterion regarding material ductility depends on the compressive strength and strain of the concrete.

The model is orthotropic in the principal stress directions for the biaxial state of stress: In order to scale the model to one-dimensional experiments, equivalent uniaxial strain increments $d\varepsilon_{iu}$, $i = 1, 2$, in the principle axes i are employed throughout. For such quantities the stress-strain law decouples

$$\begin{pmatrix} d\sigma_1 \\ d\sigma_2 \\ d\tau_{12} \end{pmatrix} = \begin{pmatrix} E_1 & 0 & 0 \\ 0 & E_2 & 0 \\ 0 & 0 & G \end{pmatrix} \cdot \begin{pmatrix} d\varepsilon_{1u} \\ d\varepsilon_{2u} \\ d\gamma_{12} \end{pmatrix}, \tag{1}$$

with

$$d\varepsilon_{1u} = \frac{1}{1-\nu^2}\left(d\varepsilon_1 + \nu \sqrt{\frac{E_2}{E_1}} d\varepsilon_2 \right), \tag{2}$$

$$d\varepsilon_{2u} = \frac{1}{1-\nu^2}\left(d\varepsilon_2 + \nu \sqrt{\frac{E_1}{E_2}} d\varepsilon_1 \right). \tag{3}$$

Because of the diagonal material matrix in (1), which implies a uniaxial behaviour, the strains ε_{iu} are also given as equivalent uniaxial values. Obviously, incremental constitutive laws

$$d\varepsilon_{iu} = \frac{d\sigma_i}{E_i} \tag{4}$$

are derived from (1), which lead to those for the finite internal variables:

$$\varepsilon_{iu} = \int \frac{d\sigma_i}{E_i} \approx \sum^{Nload} \frac{\Delta\sigma}{E_i}, \quad i = 1, 2. \tag{5}$$

Because of the lack of information about the shear modulus under general biaxial stress, the shear modulus is determined such that no particular direction is favoured. This postulate is met if the shear modulus G is not changed by transformation of reference axes. Thus the shear modulus G is determined as

$$(1-\nu^2)G = \frac{1}{4}(E_1 + E_2 - 2\nu\sqrt{E_1 E_2})\,. \tag{6}$$

The stiffness matrix and internal force vector evaluated in the principal stress system then has to be further transformed into the convective coordinate system.

Concrete in compression The stress-strain relationship is defined in the principal stress directions *i* using equivalent uniaxial strains. Here a constitutive law originally published by Saenz (1964) was used

$$\sigma_i = \frac{\varepsilon_{iu} E_0}{1 + \left[\frac{E_0}{E_S} - 2\right]\frac{\varepsilon_{iu}}{\varepsilon_{ic}} + \left[\frac{\varepsilon_{iu}}{\varepsilon_{ic}}\right]^2}, \quad 0 \geq \varepsilon_{iu} \geq \varepsilon_{ic}\,. \tag{7}$$

The strain softening branch, $\varepsilon_{iu} \leq \varepsilon_{ic}$, starts as a straight line at σ_{ic} and ends with $0.2\sigma_{ic}$ at $\varepsilon_{iu} = (1 + n)\varepsilon_{ic}$, where n varies from 1.2 to 3.0 depending on the compressive strength according to MC 90 (1990).

Concrete in tension The behaviour of concrete in tension prior to cracking is assumed linear elastic. The formation of tension cracking is described by a principle stress criterion of Rankine type. After cracks have been formed, the force in the concrete is taken by the steel reinforcement. The tension-softening range is modelled by assigning modified stiffness properties to the reinforcement steel. The stiffness of concrete perpendicular to the crack is set to zero and a uniaxial state develops in the principal stress system. If a tension crack already exists, a second crack may develop perpendicularly to the first one. Depending on the load and deformation history of the structure, the directions of cracks rotate according to the principal strain directions. Some cracks may close again due to local unloading or changing of the load direction (Swinging Crack Model or Rotating Crack Model). The crack-closing process is formulated based on Su & Zhu (1994) getting for the initial re-contact of the crack flanks the strain ε_{irc}:

$$\varepsilon_{irc} = \varepsilon_p + 0.5\varepsilon_{\max}\left(0.1 + \frac{0.9\varepsilon'_{ic}}{\varepsilon'_{ic} + \varepsilon_{\max}}\right), \tag{8}$$

$$\varepsilon'_{ic} = |\varepsilon_{ic}| - |\varepsilon_p| \geq 0\,, \tag{9}$$

with the plastic strain ε_p and for the required contact stress σ_{con}:

$$\sigma_{con} = 0.3\sigma_{ic}\left(2 + \frac{\frac{\bar{\varepsilon}_{icr}}{\varepsilon_{ic}} - 4}{\frac{\bar{\varepsilon}_{icr}}{\varepsilon_{ic}} + 2}\right) \leq \sigma_{con,\max} = \sigma_{ic}\frac{\bar{\varepsilon}_{icr}}{\bar{\varepsilon}_{icr} + \varepsilon_{ic}}, \quad \text{with} \quad \bar{\varepsilon}_{icr} = \varepsilon_{irc} - \varepsilon_p. \tag{10}$$

As Fig. 4 shows, the straight line through the points (ε_{irc}, 0) and (0, σ_{con}) with extension to the monotonic compression curve (7) describes the crack-closure path. The entire model is described in Noh (2001) in detail.

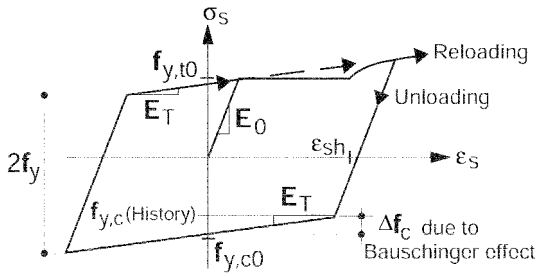

Fig. 5 Constitutive law of reinforcement steel

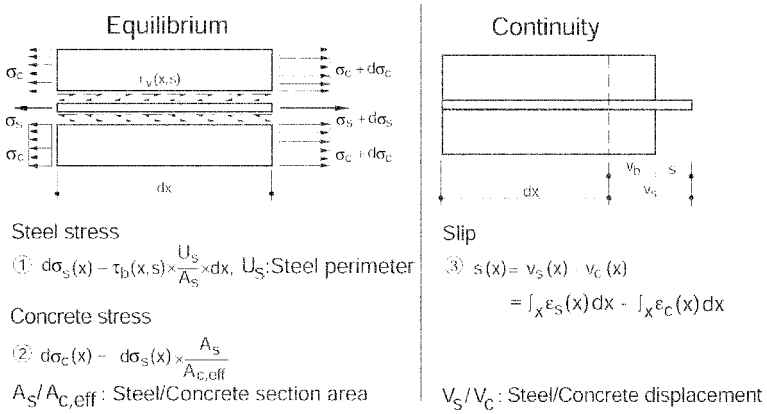

Fig. 6 Basic conditions for stresses in steel and concrete and for bond-slip

3.3 Reinforcement model and modification for considering the bond effect

The reinforcement steel is idealized as smeared in the layered shell element pictured in Fig. 3. In contrast to the concrete, reinforcement steel shows a relatively simple material behaviour. In the present work the incremental uniaxial elasto-plastic constitutive law of Fig. 5 is applied taking kinematic hardening due to Prager as well as the Bauschinger effect into account.

The bond between concrete and reinforcement plays an important role for the response of reinforced concrete structures under tensile stresses. For the present investigation the bond effect is modelled indirectly as a participation of the concrete between the cracks (tension-stiffening) by modifying the steel model both for monotonic and for unidirectional cyclic loading.

The basic relations of this one-dimensional stress transfer process are elucidated in differential elements in Fig. 6. From the condition of equilibrium we obtain

$$d\sigma_s(x) = \tau_b(x,s)\frac{U_s}{A_s}dx \tag{11}$$

$$d\sigma_c(x) = -\tau_b(x,s)\frac{U_s}{A_c}dx \tag{12}$$

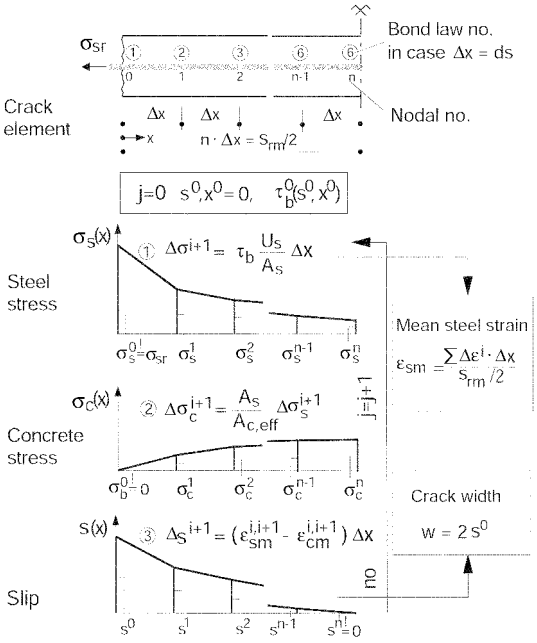

Fig. 7 Computation concept of bond effect

and the continuity condition yields for the bond-slip $s(x)$

$$s(x) = v_s(x) - v_c(x). \tag{13}$$

From the differential relations given above and shown in Fig. 6 we are now able to describe the behaviour of a crack element with length of half the crack distance $s_{rm}/2$ as depicted in Fig. 7. By introduction of suitable bond laws and integration over the length of the crack element, we are able to derive from Eqs. (11)-(13) for the steel stress, concrete stress and bond slip as follows:

$$\sigma_s(x) = \sigma_s(x = 0) + \frac{U_s}{A_s}\int_{x=0}^{s_{rm}/2} \tau_b(x, s)dx, \tag{14}$$

$$\sigma_c(x) = \sigma_c(x = 0) - (\sigma_s(x) - \sigma_s(x = 0))\frac{A_s}{A_c}, \tag{15}$$

$$s(x) = \int_{x=0}^{s_{rm}/2} \varepsilon_s(x)dx - \int_{x=0}^{s_{rm}/2} \varepsilon_c(x)dx. \tag{16}$$

For the model set-up, an iterative computation concept in the meso-level with the step-by-step integration of Eligehausen (1983) was employed, which allows the use of any arbitrarily complicated bond law (Fig. 7). For monotonic loading, the bond model of Kreller (1990) in Fig. 8 was employed, which is also valid for large slip, e.g., in the case of yielding of the reinforcement. For cyclic loading, the bond model of Tue (1993) is used, being more adequate for the service load state compared to the cyclic bond models described in CEB 210 (1991).

For an efficient computation only some characteristic points in the macro-level in Fig. 9 are

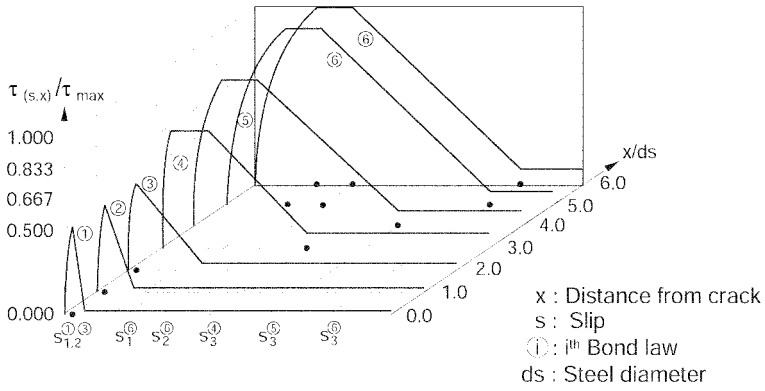

Fig. 8 Bond-slip relationship according to Kreller (1990)

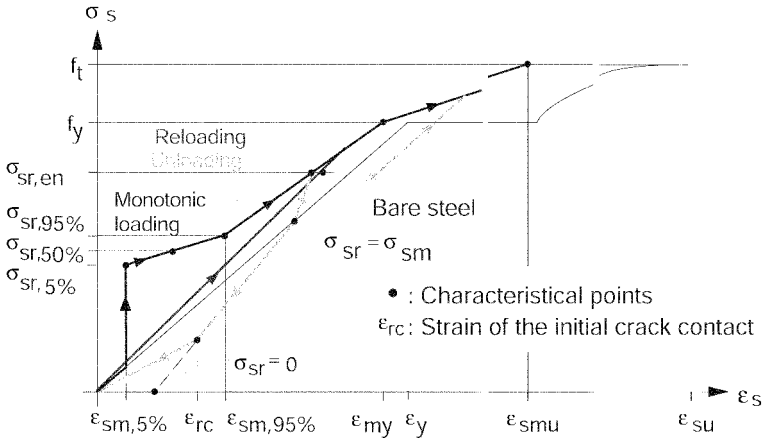

Fig. 9 Modified model of reinforcement steel

determined. In each respective point, either the stress or the strain is a known value and the other one has to be evaluated. Thereby the stress is determined in the cracked section, while the computed strain is the mean value between cracks. The linear connection of these points describes the modified reinforcement model.

The crack spacing which is assumed as known for the estimation of the mean strain can be determined from Kreller (1990). Here, a normal distribution of the tensile strength is assumed and the extent of crack formation is considered. In relation to the transfer length l_e under consideration of the scattering tensile strength in a grade of crack formation ξ the average crack spacing s_{rm} results from

$$s_{rm}(\xi) = \frac{1}{\xi} \cdot (2.0 - 0.69 \cdot \xi) \cdot l_e(\xi/2), \quad \text{with} \quad 0 \le \xi \le 1. \tag{17}$$

For plane-stress the principal mechanisms of stress transfer between steel and concrete remain unchanged. Only for the determination of the crack spacing it is assumed that the main loading reinforcement with crack spacing according to (17) specifies the crack spacing in this primary

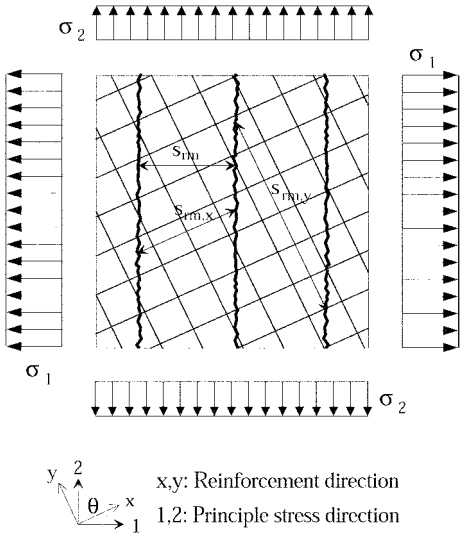

Fig. 10 Assumption of crack spacing in 2D

reinforcement direction, e.g. in *x*- direction, $s_{rm,x}$ (Fig. 10). Thus the crack spacing s_{rm} and this in the secondary reinforcement direction $s_{rm,y}$ results respectively from

$$s_{rm} = \cos\Theta \cdot s_{rm,x}, \quad s_{rm,y} = \frac{s_{rm,x}}{\tan\Theta}. \tag{18}$$

4. Damage analysis of large cooling towers

4.1 Introduction

The cooling tower analysed in the following has the same geometry as the Niederaussem Tower (Busch *et al.* 2002), however the above mentioned special considerations in section 2 are regarded in a generalised way. Fig. 11 gives the dimensions of the structure with its varying shell thickness over the height. On the right side in the figure, the necessary amount of reinforcement steel is pictured which resulted from linear analysis according to VGB (1997). The geometry of the shell consisting of two hyperbolic shells is described by Eq. (18) using the parameters in Tab. 1:

$$r(z) = r_0 + \frac{a}{b}\sqrt{b^2 + (H_T - z)^2}. \tag{19}$$

48 radial piers on the foundations ($D/B/H$ = 5.00 m/7.00 m/3.50 m) support the shell. A pier was constructed with a constant width of 1.40 m and a linearly decreasing depth from 3.10 m to 1.10 m over the height. The foundations are simulated as springs with an assumed Winkler modulus of 12.00 MN/m^3. The used concrete and reinforcement steel are assumed as B 35 and BSt 500S according to German Standard DIN 1045. Additionally the variation coefficient of the tensile strength of the concrete is assumed as 10%. For the reinforcement steel the tangent stiffness in the

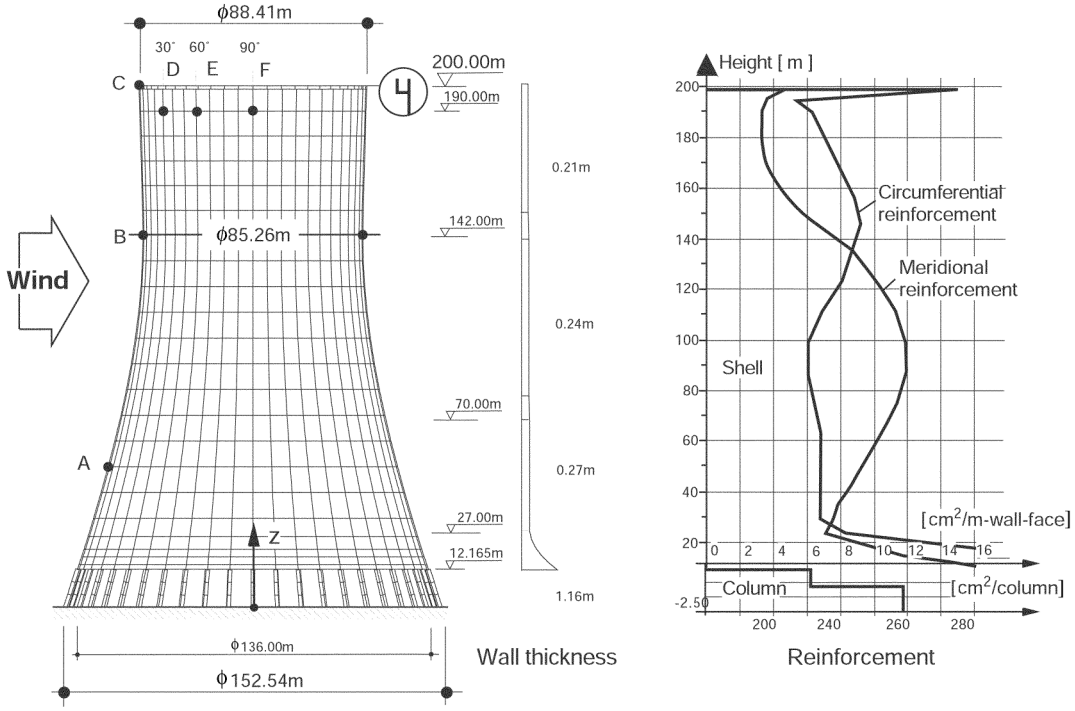

Fig. 11 Overview of the analysed prototype

yield range is assumed 10^{-3} times the initial stiffness E_0 and the fracture strain was defined as 0.1.

According to VGB the tower is subjected to dead weight G, quasi-static wind load W of wind zone II with the wind pressure distribution curve K 1.4, and alternatively to temperature loads due to winter service conditions with a temperature difference of 45 K from the cooler outer to the warmer inner face. In addition, the hygric effect of swelling on the inner face due to permanent wetting and shrinkage on the outer face were substituted by a temperature load. A reasonable assumption according to German Standard DIN 4227 results in an equivalent temperature gradient of 15 K for a nearly 30 years old tower.

4.2 Static analysis

Fig. 12 and Fig. 13 show the deformation curves at the point of throat in the stagnation meridian and a point in the flank, which are pictured as Point B and E in Fig. 11, respectively. As already recognised by the crack damage simulations of several cooling towers (Noh 2001, Krätzig *et al.* 1992) the processes of crack formation in large cooling tower shells are in principal quite similar: Without thermal service loads the shell behaves linearly up to a wind load factor, in this case λ=1.20, at which the tensile stress of the concrete in the luff regions reaches the tensile strength. Beyond this load level, cracks form and develop horizontally on the luff side as well as vertically on the flanks, successively. The cracks propagate and join together with increasing wind load. Compared to that, the temperature load ΔT_{45K} under winter service condition leads to cracks on the whole outer face of the shell. The hygric effect increases the grade of this initial crack damage,

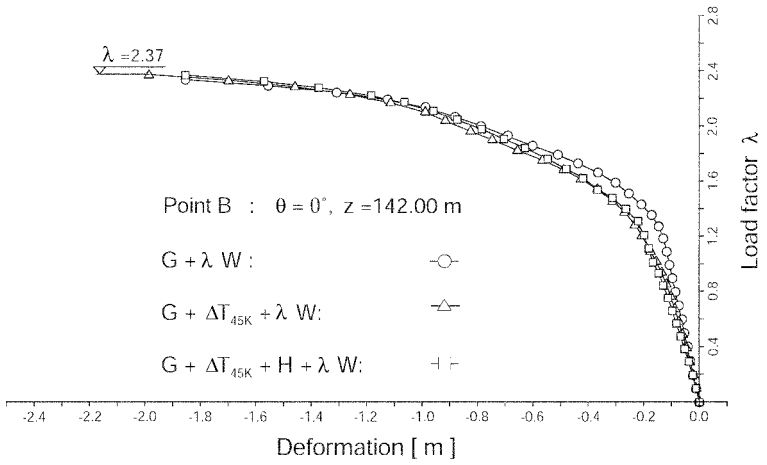

Fig. 12 Load-deflection curves at point B

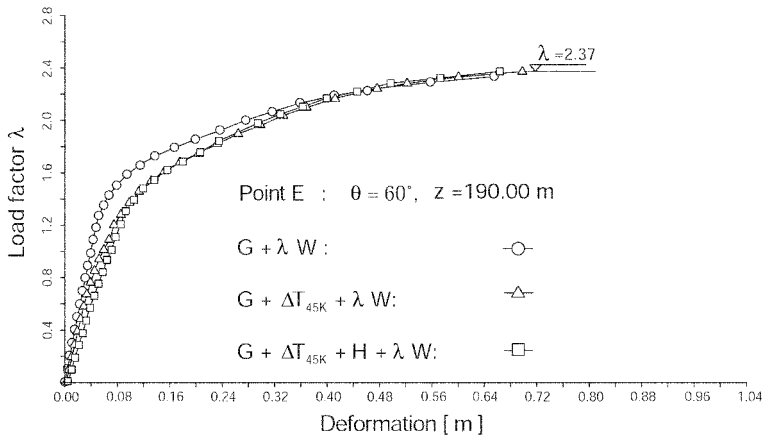

Fig. 13 Load-deflection curves at point E

leading particularly to circumferential bending damage due to meridional cracks in the flank regions. This temperature and hygric effect play an important role for further damage processes under service load. This initial damage however tends to be reduced with increasing wind load factor and finally the wind load alone determines the collapse behaviour of the tower. On this account, the tower approximately collapses at the same wind load factor, in this case $\lambda = 2.37$, in all three load cases investigated.

In Fig. 14 crack patterns on the outer face under wind load factor $\lambda = 2.00$ for the investigated load combinations are exemplarily pictured. For clearness, the cracks under thermal and hygric effects are represented only for the width > 0.1 mm and > 0.15 mm. The comparison of the crack patterns shows the influences of thermal and hygric effects on the crack damage of the shell.

It is noticeable that the tower shows an acceptable crack-behaviour in the analysis: The typical crack pattern with remarkable meridional cracks is not observed. Only a few cracks are wider than the limit of 0.2 mm. This results in the new recommendation in VGB (1997) for the minimum

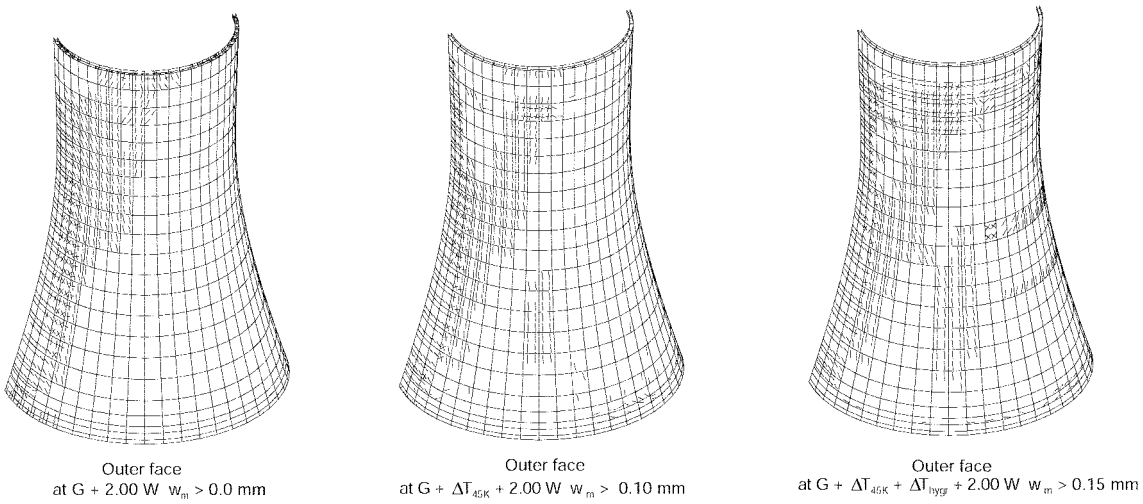

Fig. 14 Comparison of crack patterns under $\lambda = 2.00$

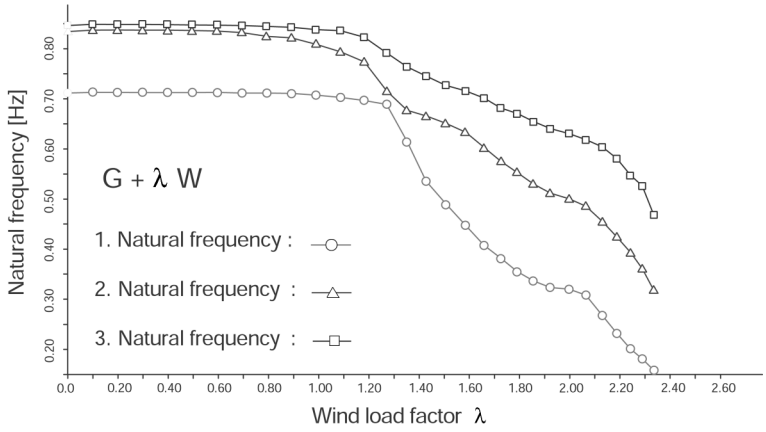

Fig. 15 Shift of the first 3 natural frequencies under $G + \lambda W$

reinforcement ration of 0.4% in the meridional direction of the upper shell.

4.3 Vibration analysis

The stiffness reduction of structures during the damage process influences its vibration characteristics. In the numerical analysis this obviously affects the stiffness matrix K_T. The most succinct form of damage information in K_T corresponds to the structureís natural frequencies. Fig. 15 shows the decrease of the first three natural frequencies as a function of the wind load factor λ for the load combinations treated already in the static analysis above. Under the load combination $G+\lambda W$ the first natural frequency, about $f = 0.70$ Hz, remain approximately constant up to the occurrence of the successive formation of horizontal cracks on the luff side at $\lambda = 1.30$. Afterwards the first one drops dramatically until the collapse of the tower occurs, whereas the second and third

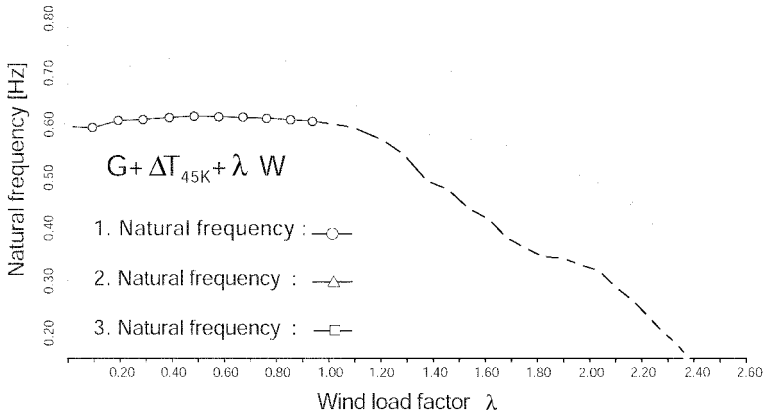

Fig. 16 Shift of the first 3 natural frequencies under $G + \Delta T_{45K} + \lambda W$

ones react stronger than the first one under lower intensity of wind loads. The reduction of the stiffness due to temperature decreases the natural frequencies considerably. The first natural frequency $f = 0.71$ Hz reduces to $f = 0.59$ Hz due to temperature load alone. The result of the analysis due to additional hygric effects can be found in Noh (2001). Thereby it is found that the first one decreases to $f = 0.53$ Hz under an additional hygric effect. Under the load combination $G + \Delta T_{45K} + \lambda W$ in Fig. 16, the three natural frequencies demonstrate basically the same behaviors.

In Fig. 17 the shifted first three natural modes of the investigated damage states are presented for the some wind intensities in combination with thermal load ΔT_{45K}. The undamaged tower has its first three natural modes with 5, 3 and 4 waves respectively. However, after the formation of cracks on the whole outer face of the tower due to the temperature load, the new second mode with a reduced natural frequency of $f = 0.68$ Hz now has 6 waves. At the wind load level $\lambda = 1.20$ at which the second natural frequency drops sharply, the second mode has 5 waves. From this load level onwards, the first mode is quite similar to the deformation pattern of the structure. At a load level close to collapse, the second and third modes also tend to assume a form similar to the deformation of the cracked structure: The deformation pattern under the given crack-damage state of the structure can be obtained easily. The evaluations of natural frequencies and natural modes under consideration of the hygric effect show in principle the same behaviour (Noh 2001).

The determination of the evolution of natural frequencies during the damage process makes it possible to estimate the increase of the wind excitation level in a simplified manner. If the varying first natural frequencies under increasing loads are registered into the Von-Kármán-spectrum, one confirms wind- and temperature-induced shifts of the first natural frequencies from their virgin positions towards the spectral peak. For plane and open ground e.g., the spectral density S of natural wind:

$$\frac{S(f) \cdot f}{\sigma^2} = \frac{4 \cdot f^*}{[1 + (8.409 \cdot f)^2]^{5/6}}, \tag{20}$$

defined with the frequency f, variance σ, and the reduced frequency f^* depending on the height and type of the ground, increases about 17% and 24% respectively. Furthermore, the increase of the wind load intensity can be estimated by about 32% at the load case $G + \Delta T_{45K} + 1.40W$. One can

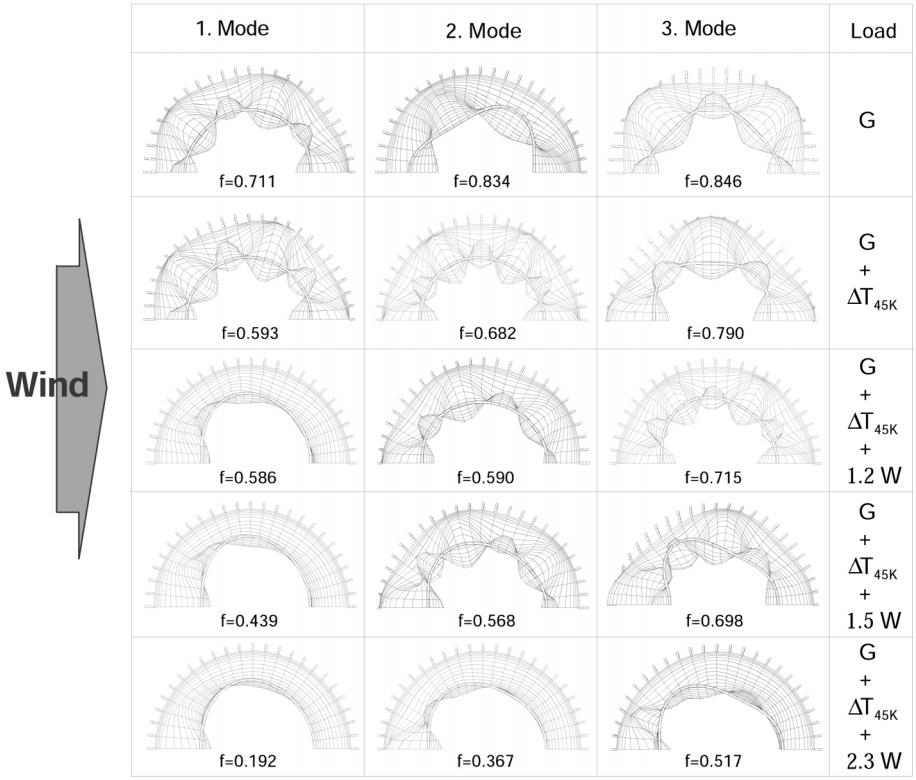

Fig. 17 Shift of the first 3 natural modes under $G + \Delta T_{45K} + \lambda W$

Table 1 Parameters for the shell geometry

	r_0 [m]	a [m]	b [m]	H_T [m]
Upper shell	–7.2435	49.8735	114.9326	142.00
Lower shell	42.3703	0.2597	8.2940	142.00

deduce from the increase of the spectral excitation level an approximately equally large increase of the internal stresses and of the crack damages respectively. In such way the structural response can be shifted to more energetic ranges of the wind-spectrum, thus again enhancing the dynamic wind action accumulatively. Consequently the structure is subjected to the progressive damage process.

5. Conclusions

The paper demonstrates the new design concept performed successfully for the world's largest cooling tower at Niederaussem. The cooling tower has been completed in 2000 and operates since middle of 2002 (Fig. 2). This new tower with a series of innovative design elements and with a durability-oriented concept will contribute to a highly efficient electric energy unit with savings of more than 30% of fossil fuel compared to power stations of the eighties, and thus further

minimizing environmental pollution.

The paper also shows the progressive damage process of natural draught cooling towers. This damage process results, under wide-band excitation, from a shift of the structural response spectrum towards higher excitations, caused by degrading structural stiffness and also a damage-controlled self-adaptation phenomenon. The damage processes develop progressively over the life-cycle of the structure and cause a reduction of the originally expected life duration. This numerical consideration is surely advantageous for the proof of sufficient safety against the ultimate limit state as well as for the understanding of damage mechanisms for the improvement of durability and for extension of the life-cycle of structures subject to such damage processes.

References

Busch, D., Harte, R., Krätzig, W.B. and Montag, U. (2002), "New natural draught cooling tower of 200 m of height", *Eng. Struct.*, **24**, 1509-1521.

Busch, D., Haselwander, B., Hillemeier, B. and Strauß, J. (1999), "Innovative Betontechnologie für den Kühlturmbau", *beton.*, 1999:**4**, 108-109.

CEB 210 (1991), *Behaviour and analysis of reinforced concrete structures under alternate actions inducing inelastic response-volume 1, CEB Bulletin d'Information 210* Comité Euro-International du Béton, Lausanne.

Darwin, D. and Pecknold, D.A. (1974), "Inelastic model for cyclic biaxial loading of reinforced concrete", Civil Engineering Studies SRS Nr. 409, University of Illinois.

Eligehausen, R., Popov, E.P. and Bertero, V.V. (1983), "Local bond stress-slip relationships of deformed bars under generalized excitations", College of Engineering, University of California.

Harte, R., Krätzig, W.B., Noh, S.-Y. and Petryna, Y.S. (2000), "On progressive damage phenomena of structures", *Comput. Mech.*, **25**, 404-412.

Harte, R. and Krätzig, W.B. (2002) "Large-scale cooling towers as part of an efficient and cleaner energy generating technology", *Thin-Walled Structures*, **40**, 651-664.

Karsan, D. and Jirsa, J.O. (1969), "Behavior of concrete under compressive loadings", *J. Struct. Div.*, ASCE, **95**(ST12), 2543-2563.

Krätzig, W.B., Gruber, K. and Zahlten, W. (1992), "Numerical collapse simulation of large cooling towers checking their safety and durability", Technical Report 92-3 Ruhr-University Bochum.

Krätzig, W.B. (1997), "Multi-level modelling techniques for elasto-plastic structural responses.", Owen D.R.J., Onate E. and Hinton E. (editors). *Computational plasticity, Part 1. Int. Center for Num. Meth. Engng*. Barcelona, Spain, 457-468.

Krätzig, W.B., Meskouris, K. and Noh, S.-Y. (2001) "On damage process of natural draught cooling towers", Eds.: W.A. Wall *et al.*, *Proc. Int. Conf. Trends in Computational Structural Mechanics*, 338-347, CIMNE, Barcelona, Spain.

Kreller, H. (1990), *Zum nichtlinearen Trag- und Verformungsverhalten von Stahlbetonstabtragwerken unter Last- und Zwangeinwirkung*, Deutscher Ausschuß für Stahlbeton Heft 409.

Kupfer, H.B., Hilsdorf, H.K. and Rüsch, H. (1969) "Behavior of concrete under Biaxial Stresses", *ACI J.*, **66**(8), 656-666.

MC 90 (1990), *CEB-FIP Model CODE 1990 Design Code, Bulletin d'Information 195*, Comité Euro-International du Béton, Lausanne.

Menzel, W. (1996), *Gemischt-hybride Elemente Formulierungen für komplexe Schalen- strukturen unter endlichen Rotationen*, TWM Nr.96-4, Institut für Konstruktiven Ingenieurbau der Ruhr-Universität Bochum.

Noh, S.-Y. (2001), *Beitrag zur numerischen Analyse der Schädigungsmechanismen von Naturzugkühltürmen*, Dr.-Ing. Thesis, RWTH Aachen, Germany.

Noh, S.-Y., Krätzig, W.B. and Meskouris, K. (2002) "Numerical simulation of serviceability, damage evolution and failure of reinforced concrete shells", *Comput. Struct.*, in print.

Saenz, I.P. (1964), Discussion to "Equation for the stress-strain curve of concrete by Desayi and Krishnan", *ACI*

J., **61**(9), 1229-1235.
Su, X. and Zhu, B. (1994), "Algorithm for hysteresis analysis of prestressed-concrete frames", *J. Struct. Eng.*, **120**(6), 1732-1744.
Tue, N.V. (1993), *Zur Spannungsumlagerung im Spannbeton bei der Rißbildung unter statischer und wiederholter Belastung*, Deutscher Ausschuß für Stahlbeton Heft 435.
VGB-Guidelines (1997), "Structural design of cooling towers", VGB-Technical Committee Essen, Germany.